Pergamon

www.neuroscience-ibro.com

PII: S0306-4522(01)00440-7

Neuroscience Vol. 109, No. 1, pp. 63–80, 2002

0306-4522/02 $22.00+0.00

CHOLECYSTOKININ-IMMUNOPOSITIVE BASKET AND SCHAFFER COLLATERAL-ASSOCIATED INTERNEURONES TARGET DIFFERENT DOMAINS OF PYRAMIDAL CELLS IN THE CA1 AREA OF THE RAT HIPPOCAMPUS

D. W. COPE,* G. MACCAFERRI,[1] L. F. MÁRTON, J. D. B. ROBERTS, P. M. COBDEN and P. SOMOGYI

MRC Anatomical Neuropharmacology Unit, Department of Pharmacology, Oxford University, Mansfield Road, Oxford OX1 3TH, UK

Abstract—Two types of GABAergic interneurone are known to express cholecystokinin-related peptides in the isocortex: basket cells, which preferentially innervate the somata and proximal dendrites of pyramidal cells; and double bouquet cells, which innervate distal dendrites and dendritic spines. In the hippocampus, cholecystokinin immunoreactivity has only been reported in basket cells. However, at least eight distinct GABAergic interneurone types terminate in the dendritic domain of CA1 pyramidal cells, some of them with as yet undetermined neurochemical characteristics. In order to establish whether more than one population of cholecystokinin-expressing interneurone exist in the hippocampus, we have performed whole-cell current clamp recordings from interneurones located in the stratum radiatum of the hippocampal CA1 region of developing rats. Recorded neurones were filled with biocytin to reveal their axonal targets, and were tested for the presence of pro-cholecystokinin immunoreactivity.

The results show that two populations of cholecystokinin-immunoreactive interneurones exist in the CA1 area ($n=15$ positive cells). Cholecystokinin-positive basket cells (53%) preferentially innervate stratum pyramidale and adjacent strata oriens and radiatum. A second population of cholecystokinin-positive cells, previously described as Schaffer collateral-associated interneurones [Vida et al. (1998) J. Physiol. 506, 755–773], have axons that ramify almost exclusively in strata radiatum and oriens, overlapping with the Schaffer collateral/commissural pathway originating from CA3 pyramidal cells. Two of seven of the Schaffer collateral-associated cells were also immunopositive for calbindin. Soma position and orientation in stratum radiatum, the number and orientation of dendrites, and the passive and active membrane properties of the two cell populations are only slightly different. In addition, in stratum radiatum and its border with lacunosum of perfusion-fixed hippocampi, 31.6 ± 3.8% (adult) or 26.8 ± 2.9% (postnatal day 17–20) of cholecystokinin-positive cells were also immunoreactive for calbindin.

Therefore, at least two populations of pro-cholecystokinin-immunopositive interneurones, basket and Schaffer collateral-associated cells, exist in the CA1 area of the hippocampus, and are probably homologous to cholecystokinin-immunopositive basket and double bouquet cells in the isocortex. It is not known if the GABAergic terminals of double bouquet cells are co-aligned with specific glutamatergic inputs. However, in the hippocampal CA1 area, it is clear that the terminals of Schaffer collateral-associated cells are co-stratified with the glutamatergic input from the CA3 area, with as yet unknown functional consequences. The division of the postsynaptic neuronal surface by two classes of GABAergic cell expressing cholecystokinin in both the hippocampus and isocortex provides further evidence for the uniform synaptic organisation of the cerebral cortex.

Key words: cholecystokinin, cortex, inhibition, GABA, calbindin.

The synaptic organisation of the hippocampal formation demonstrates that the surface of cortical neurones is subdivided by both extrinsic and intrinsic inputs into several functional domains (Ramon y Cajal, 1893; for reviews see Freund and Buzsáki, 1996; Somogyi et al., 1998). Distinct GABAergic interneurones innervate the soma, axon initial segment or dendritic zones of pyramidal cells. In the dendritic domains, the inter-areal and local glutamatergic, and the local GABAergic, inputs target select regions and are frequently co-aligned (Ramon y Cajal, 1893; Gulyás et al., 1993; Han et al., 1993; Buhl et al., 1994a; Vida et al., 1998). The conspicuous constraints in the placement of synapses on the neuronal surface predict distinct functional roles of interneurones with different target selectivity. Many roles, including feed-forward, feed-back, tonic and lateral inhibition,

[1] Present address: Department of Pharmacology, Emory University School of Medicine, Atlanta, GA 30322, USA.

*Corresponding author. Tel.: +44-1865-271898; fax: +44-1865-271648.

E-mail address: david.cope@pharm.ox.ac.uk (D. W. Cope).

Abbreviations: aCSF, artificial cerebrospinal fluid; ADP, after-depolarisation; AHP, after-hyperpolarisation; AMCA, 7-amino-4-methylcoumarin-3-acetic acid; CB1, cannabinoid receptor type 1; CCK, cholecystokinin; EPSPs, excitatory postsynaptic potentials; fAHP, fast after-hyperpolarisation; HEPES, *N*-(2-hydroxyethyl)piperazine-*N*′-(2-ethanesulphonic acid); HRP, horseradish peroxidase; IPSPs, inhibitory postsynaptic potentials; ISI, interspike interval; mAHP, medium-duration after-hyperpolarisation; P, postnatal day; PV, parvalbumin; R_N, input resistance; τ_m, membrane time constant; TBS, Tris-buffered saline; V_h, holding membrane potential; VIP, vasoactive intestinal polypeptide; V_m, resting membrane potential.

temporal phasing of pyramidal neurones, prevention of input saturation and control of dendritic Ca^{2+} electrogenesis, have been suggested, requiring distinct populations of GABAergic cells (for review see McBain and Fisahn, 2001). To assign distinct functions to groups of interneurones requires a rigorous definition of their identity, based on functionally relevant criteria such as synaptic input/output characteristics and molecular markers. In spite of considerable effort, there is no agreement on the number of distinct neuronal populations even in such an extensively studied cortical area as the hippocampal formation.

The most frequently used features for determining cell identity have been: (i) their intrinsic biophysical parameters and positions within cortical laminae, (ii) the source of their synaptic inputs, (iii) the target destination of their axon, (iv) their neurotransmitter receptor expression and agonist sensitivity, and (v) the expression of neurochemical markers, such as neuroactive peptides and Ca^{2+}-binding proteins (Kawaguchi and Hama, 1987, 1988; Kosaka et al., 1987; Buhl et al., 1994a; Sik et al., 1995; Miles et al., 1996; Hájos and Mody, 1997; Nomura et al., 1997; Ali and Thomson, 1998; Parra et al., 1998; Vida et al., 1998; Ali et al., 1999; Maccaferri et al., 2000; for review see Freund and Buzsáki, 1996). These characteristics have not been completely aligned to each other, sometimes due to technical limitations. The lack of direct information on the same individual cells has led to views that only very few distinct non-overlapping classes of cell exist, or to suggesting novel classes of cell based only on a limited range of determined or assumed properties. Nevertheless, a direct determination of several features of the same individual cell, in particular axonal target patterns and neurochemical properties, has provided clear delineation of GABAergic neurones with non-overlapping properties. Firstly, two types of basket cell, which express either parvalbumin (PV) (Kawaguchi et al., 1987; Kosaka et al., 1987; Katsumaru et al., 1988) or cholecystokinin (CCK) and vasoactive intestinal polypeptide (VIP) (Harris et al., 1985; Hendry and Jones, 1985; Kosaka et al., 1985; Nunzi et al., 1985; Acsády et al., 2000), and have axons targeting preferentially the soma and proximal dendrites of pyramidal neurones, have been identified. Secondly, axo-axonic cells target specifically the axon initial segment of pyramidal neurones, and express PV (Somogyi, 1977; Kosaka et al., 1985; Katsumaru et al., 1988). Thirdly, GABAergic cells that innervate distal dendrites and spines of pyramidal neurones show the greatest diversity and express individually, or in combination, somatostatin, neuropeptide Y, enkephalin and/or calbindin (for review see Freund and Buzsáki, 1996). And lastly, interneurone subtypes that mostly innervate other interneurones express either VIP and/or calretinin (Acsády et al., 1996; Gulyás et al., 1996).

The above described principles appear to apply throughout the cortical mantle, as far as they have been examined, but not surprisingly some differences between different cortical areas appear to exist. For example, in the isocortex two types of CCK-expressing GABAergic interneurones have been described, based on their different synaptic target selection (Freund et al., 1986). As in the hippocampus, one population appears to target preferentially the soma and proximal dendrites of postsynaptic neurones and hence are called basket cells (Peters et al., 1983; Freund et al., 1986; Kawaguchi and Kubota, 1997, 1998). Another population of CCK-expressing neurones in the isocortex has characteristic interlaminar axon bundles which make synapses with more distal dendrites and dendritic spines of pyramidal cells or other interneurones, and are called double bouquet cells (Somogyi and Cowey, 1981; Freund et al., 1986). At least eight classes of interneurones that target the distal dendritic domains of CA1 pyramidal cells alone have been identified. The cell bodies of these cells are located throughout all layers, but whether any of them express CCK has not been tested. In conjunction, the cell bodies of CCK-expressing interneurones are scattered throughout the hippocampal layers with some tendency of concentration at the strata radiatum/lacunosum-moleculare border (Greenwood et al., 1981; Somogyi et al., 1984; Harris et al., 1985; Hendry and Jones, 1985; Nunzi et al., 1985). Several interneurones have been reported which have somata outside stratum pyramidale but densely innervate the pyramidal layer, and are therefore considered basket cells. Because PV-expressing basket cell bodies are located exclusively in strata pyramidale and oriens (Kosaka et al., 1987), the basket cells located in the other strata are likely to express CCK, but this has been directly proven for only one cell located in stratum oriens (Maccaferri et al., 2000). It is probable that some of the CCK-expressing interneurones at the strata radiatum/lacunosum-moleculare border are also basket cells. However, it is not known if they are solely representative of basket cells, or whether cells with a dendritic target preference also exist.

To test whether CCK-expressing interneurones in the CA1 region of the hippocampus could include a population that targets distal dendrites, we have electrophysiologically recorded from interneurones located in stratum radiatum of the CA1 area. Subsequently, the cells were immunocytochemically tested for the presence of CCK using antibodies that recognise the pro-CCK protein (Morino et al., 1994), and are therefore particularly suitable for labelling cell bodies. Recorded neurones were classified on the basis of their axonal pattern revealed by biocytin labelling. The results show that, similar to the isocortex, two distinct populations of CCK-expressing interneurones exist in the CA1 area, adding further evidence to the uniform synaptic organisation of the cerebral cortex (Szentágothai, 1975, 1978).

EXPERIMENTAL PROCEDURES

All the procedures involving experimental animals were carried out in accordance with the UK Animals (Scientific Procedures) Act, 1986, and associated guidelines. All efforts were made to minimise stress to the animals and the number of animals used.

Slice preparation and electrophysiological recording

Slices of rat hippocampus were prepared as described previously (Maccaferri et al., 2000). In brief, juvenile male Wistar rats (postnatal day P11–P17) were anaesthetised using isoflurane and decapitated, or killed by cervical dislocation (Schedule 1 of The Animals (Scientific Procedures) Act, 1986). The brain was rapidly removed and adhered to the cutting stage of a vibratome (Leica Instruments, Germany) and 300 μm thick horizontal sections of hippocampus cut in continuously oxygenated (95% O_2:5% CO_2), ice-cold (~4°C) artificial cerebrospinal fluid (aCSF) of composition (in mM): NaCl 130; $NaHCO_3$ 24; KCl 3.5; NaH_2PO_4 1.25; $CaCl_2$ 1; $MgSO_4$ 3; and glucose 10. Slices were then stored at room temperature (22–25°C) in an incubation chamber for at least 1 h in continuously oxygenated aCSF of the above composition. After this time, slices were transferred to the recording chamber and perfused with warmed (35 ± 1°C), continuously oxygenated aCSF of composition (in mM): NaCl 130; $NaHCO_3$ 24; KCl 3.5; NaH_2PO_4 1.25; $CaCl_2$ 2; $MgSO_4$ 1; and glucose 10.

Both interneurones and pyramidal neurones were identified using a Zeiss Axioskop microscope (Zeiss, Germany) equipped with a 40× immersion differential interference contrast objective, coupled to an infrared camera system (Hamamatsu, Japan). Putative interneurones in stratum radiatum were identified by (i) their position within the slice, (ii) their ovoid appearance, and (iii) their lack of an obvious large apical dendrite. Whole-cell current clamp recordings were performed following acquisition of a GΩ seal (≥1 GΩ). Patch pipettes (resistance 4–10 MΩ) contained (in mM): potassium gluconate 126; KCl 4; ATP (Mg salt) 4; GTP (Na_2 salt) 0.3; phosphocreatine (Na_2 salt) 10; HEPES 10; and 0.5% biocytin. Electrodes were connected to an Axopatch-1D (Axon Instruments, USA) and data filtered at 2–5 kHz before being acquired at 10 kHz directly to computer using pClamp software via a DigiData 1200 analogue/digital converter board (both Axon Instruments). Interneurones located in stratum radiatum were electrophysiologically identified by their ability to generate high-frequency trains of short-duration, non-adapting action potentials, and the presence of a fast after-hyperpolarisation (fAHP) following termination of action potentials (for review see McBain and Fisahn, 2001). Voltage responses were elicited to hyperpolarising and depolarising current steps in increments of 25 pA at or close to resting membrane potential (V_m). Data analysis was performed using pClamp and Origin (Microcal Software, USA) software packages.

Electrophysiological analysis

Intrinsic electrophysiological properties of cells was determined in the following manner. V_m was determined following initial breakthrough into whole-cell current clamp mode, and then individual cells were injected with steady hyperpolarising or depolarising current to hold them close to −60 mV. Series resistance compensation enabled the determination of the input resistance (R_N) of each neurone in response to small (25 or 50 pA) hyperpolarising current steps. Similarly, membrane time constant (τ_m) was calculated in response to small (25 or 50 pA) hyperpolarising current steps. The presence of depolarising 'sag' potentials during the time course of long-duration hyperpolarising current steps (up to 1000 ms) was determined through calculation of the rectification ratio of peak compared to steady-state R_N for −100 pA current steps. In addition, the presence and amplitude of depolarising rebound potentials, relative to holding membrane potential (V_h), at the offset of hyperpolarising current steps was determined. In instances where rebound action potentials were generated at the offset of hyperpolarising current steps, the depolarising rebound potential was taken as the action potential firing threshold. Action potential amplitude was ascertained from firing threshold to apex of the first action potential of a low-frequency (< 10 Hz) train of action potentials, and their duration determined at half amplitude of that first action potential. The amplitude of fAHPs was measured from the firing threshold of the preceding, i.e. first, action potential in a low-frequency train of action potentials. Following the termination of the fAHP in most neurones an after-depolarising potential (ADP) occurred, the amplitude of which was calculated from the nadir of the fAHP. The amplitude of medium-duration after-hyperpolarisations (mAHPs) following ADPs was calculated from the peak of the ADP. Spike frequency accommodation was calculated by measuring the peak-to-peak inter-spike interval (ISI) of relatively high-frequency (~40 Hz) trains of action potentials. The first and last five ISIs in a spike train were averaged, as were the five ISIs closest to 200 ms into the spike train. Comparisons were then made by calculating the ratio of the mean of the first five ISIs to the mean of the last five ISIs (early-phase adaptation), and the ratio of the mean of the five ISIs closest to 200 ms to the mean of the last five ISIs (later-phase adaptation). This enabled us to determine whether spike frequency adaptation occurred primarily during the onset (first 200 ms) of the spike train, and thereafter whether it altered following the first 200 ms of firing. Although the use of an Axopatch-1D amplifier in whole-cell current clamp mode can introduce errors in the measurement of fast events, such as action potentials and fast AHPs (Magistretti et al., 1996), it does not preclude specific comparisons within this study, and general comparisons with others. All electrophysiological data are expressed as mean ± S.E.M., and Student's *t*-test was used for statistical comparison ($P < 0.05$).

Immunocytochemistry of recorded slices

Following electrophysiological recording, slices were confined between two Millipore filters to prevent slice deformation, and fixed for at least 4 h in a solution containing 4% paraformaldehyde, 1.25% glutaraldehyde and 15% (v/v) saturated picric acid in 0.1 M phosphate buffer (pH 7.4). Fixed slices were then embedded in gelatine and resectioned at 60 μm thickness. Non-specific protein binding was blocked by incubation in 20% normal goat serum for 1 h. Sections were incubated overnight (~4°C) in a mixture of rabbit polyclonal antiserum to pro-CCK (diluted 1:1000, Code L424, a gift from Dr Andrea Varro, Department of Physiology, University of Liverpool; see Morino et al., 1994), mouse monoclonal antibodies to calbindin D28 (1:400, Swant, Switzerland, Code 300, ascites) and 7-amino-4-methylcoumarin-3-acetic acid (AMCA)-conjugated streptavidin (1:1000, Vector Laboratories, Burlingame, CA, USA) to visualise biocytin, all diluted in Tris-buffered saline (TBS) and 0.1% Triton X-100. The sections were subsequently washed in TBS and incubated for 2 h in a mixture of Alexa Fluor® 488-conjugated goat anti-rabbit IgG (diluted 1:1000, Molecular Probes, Leiden, The Netherlands) and Cy™3-conjugated goat anti-mouse IgG (diluted 1:400, Jackson Laboratories, West Grove, PA, USA). The sections were washed and mounted under coverslips in Vectashield (Vector Laboratories). Cells were studied using a Leica dichromatic mirror system, as described previously (Maccaferri et al., 2000), recorded on a CCD camera, analysed and displayed using the Openlab software (Improvision, Coventry, UK). Brightness and contrast were adjusted for the whole frame and no part of a frame was enhanced or modified in any way. The immunonegativity of a cell for a marker could be due to damage caused by the recording, an undetectably low level of the molecule or the genuine absence of the molecule, therefore only the positive detection of immunoreactivity is informative following extensive whole-cell recording.

Visualisation of recorded neurones using horseradish peroxidase

Following immunocytochemical processing, sections were demounted, washed in TBS and 0.1% Triton X-100 and incubated in biotinylated horseradish peroxidase (HRP) (diluted 1:100, Vector Laboratories) overnight at ~4°C. Slices were then further washed and incubated in avidin-biotinylated HRP (diluted 1:100) for at least 6 h. 3,3′-Diaminobenzidine (0.05%) was used as chromogen and 0.01% H_2O_2 as substrate in the peroxidase reaction carried out in 0.05 M Tris buffer. Sections were then dehydrated and permanently mounted on slides. The axonal and

dendritic patterns of each neurone were analysed at high magnification using an oil immersion objective. Some recovered neurones were subsequently reconstructed at a magnification of 600× from the serial 60 μm thick sections using a drawing tube.

Cholecystokinin and calbindin immunoreactivity in perfusion-fixed hippocampi

Because the recorded neurones were from developing hippocampi and many of the distinct interneurone classes to which they were compared have only been described in adult animals, we compared hippocampal pro-CCK immunoreactivity in four adult (150 g) and four developing (P17, P20) Wistar rats. The animals were deeply anaesthetised (Sagatal, pentobarbital sodium, 220 mg/kg i.p.) and killed by perfusion, first with saline, followed by a fixative of 4% paraformaldehyde, 0.05% glutaraldehyde and 15% (v/v) saturated picric acid in 0.1 M phosphate buffer (pH 7.4). The brains were dissected, and 60 μm thick vibratome sections were cut. The sections were washed in phosphate-buffered saline, and reacted as described above for recorded brain slices, except that the AMCA-conjugated streptavidin was omitted.

RESULTS

Data base

A total of 54 interneurones were recorded in stratum radiatum of the CA1 area. Of these cells, 36 were tested for the presence of pro-CCK and 22 were found to be immunopositive (Fig. 1). Of the 54 cells, 32 were tested for the presence of calbindin, all of which were also tested for pro-CCK, and only two were found to be immunopositive; both of them were also immunopositive for pro-CCK. Following development of the biocytin, 15 of the 22 pro-CCK-positive interneurones had sufficient recovered axon within the slice to establish their laminar selectivity. The data presented here therefore represent those acquired from these 15 cells.

Cholecystokinin and calbindin immunoreactivity in recorded cells

Fluorescence labelling for biocytin was present in the somata and dendrites of the recorded cells as relatively uniform, cytoplasmic labelling (Fig. 1A–D), but the axons were rarely detectable. Immunofluorescence for pro-CCK was found in the soma in discrete perinuclear patches and/or as a punctate pattern, presumably corresponding to the Golgi apparatus (Fig. 1E–H). In addition, several proximal dendrites could often be observed to contain pro-CCK-immunoreactive material. Non-recorded neurones that showed pro-CCK immunofluorescence were also apparent in all sections (e.g. Fig. 1E, H), indicating that the pro-CCK immunoreactivity was unlikely to be induced by recording. The degree of immunoreactivity was often lower in the recorded neurones than in surrounding pro-CCK-immunopositive neurones, probably caused by a lower rate of synthesis and/or the degradation of the protein due to cytoplasmic dialysis during recording. Therefore, only positive results are used as evidence for the presence of CCK in a given neurone, and the absence of immunoreactivity cannot be taken as evidence for the absence of the molecule, which may have been expressed at a low level initially and subsequently declined further in some recorded neurones. This could be a particularly likely event for cytoplasmic proteins such as calbindin, which might be dialysed by the recording electrode to undetectable level, and might explain the low detection rate in recorded neurones.

Cholecystokinin-immunopositive basket cells

Of the 15 pro-CCK-immunopositive interneurones that had sufficient recovered axon for classification, 53% ($n = 8$) were found to concentrate their axonal arbor in the pyramidal cell layer and are therefore considered to be basket cells (Fig. 2A, B). Their somata were found scattered throughout the sampled width of stratum radiatum (Fig. 3C). The soma was usually ovoid or fusiform in shape with the long axis characteristically orientated perpendicular to the strata (Figs. 1I, J and 2A, B). Between three and six primary dendrites emerged radially from the soma and the majority subsequently branched into secondary and sometimes tertiary arborisations close to the soma. The dendrites predominantly ran perpendicular to the strata, progressing throughout stratum radiatum and often reaching both strata lacunosum-moleculare and oriens. Most of the dendrites reached the surface of the slice and were truncated. The dendrites were often sparsely spiny, although aspiny ones were also infrequently seen. The axon emerged either directly from the soma, or more commonly from a proximal dendrite close to the soma, and branched extensively in stratum radiatum adjacent to stratum pyramidale, in some cases running parallel to stratum pyramidale for some distance, before entering stratum pyramidale and ramifying extensively (Fig. 2A, B). The axonal branches formed varicosities around cell bodies and along the proximal apical dendrites (Fig. 3B). In all cases basket cells also innervated, to varying degrees, strata oriens and radiatum adjacent to stratum pyramidale. Occasionally, the axon, upon arising from the soma or primary dendrite, progressed toward stratum lacunosum-moleculare before turning back on itself and mostly innervating the cell body layer (e.g. Fig. 2A).

Cholecystokinin-immunopositive Schaffer collateral-associated cells

Of the 15 pro-CCK-immunopositive interneurones that had sufficient axon recovery for classification, 47% ($n = 7$) were found to distribute their axons primarily outside the pyramidal cell layer. Two of these cells were also shown to be immunopositive for calbindin. Both the dendritic and axonal patterns of these cells were very similar to cells described in adult rats as 'Schaffer collateral-associated cells' (Vida et al., 1998; Cossart et al., 2001b), and in young rats as 'radial trilaminar cells' (Hájos and Mody, 1997). We retained the term Schaffer collateral-associated cell in the present study, because the 'trilaminar' term was originally introduced to describe significant innervation of the pyrami-

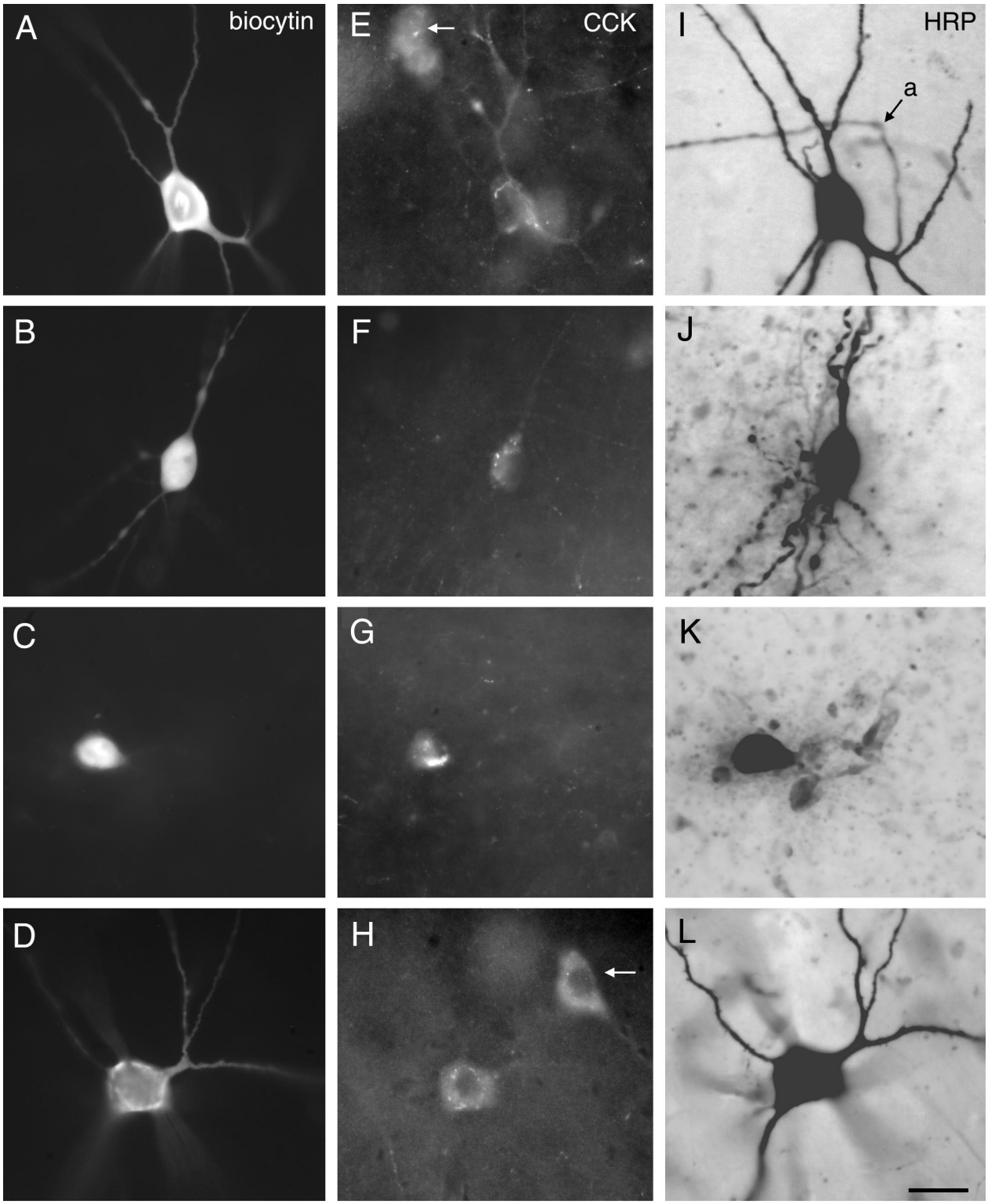

Fig. 1. Pro-CCK immunoreactivity of recorded interneurones in stratum radiatum. Four cells are shown in fluorescence images for biocytin (left panels, A–D, AMCA label) or pro-CCK (middle panels, E–H, Alexa Fluor® 488 label), and following visualisation of biocytin as HRP reaction product (right panels, I–L). (A, B) Two pro-CCK-immunoreactive basket cells whose axonal projection patterns are shown in Fig. 2. (C, D) Two pro-CCK-immunoreactive Schaffer collateral-associated cells whose axonal projection patterns are shown in Fig. 2. Arrows in E and H label non-recorded neurones which are also pro-CCK-immunopositive. Arrow in I indicates the main axon (a). Stratum pyramidale is located towards the bottom of the figures. Scale bar = 20 μm.

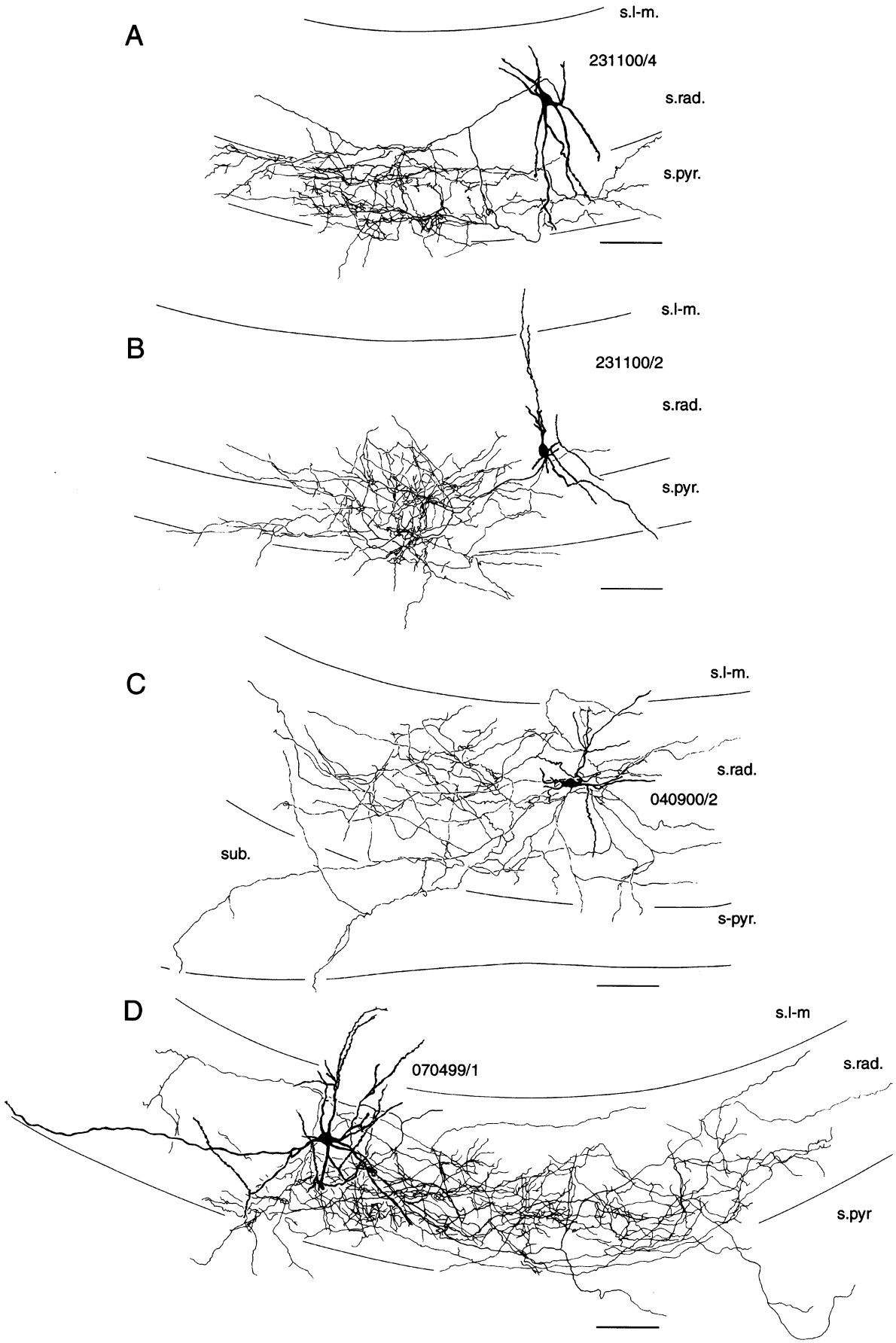
A
s.l-m.
231100/4
s.rad.
s.pyr.
B
s.l-m.
231100/2
s.rad.
s.pyr.
C
s.l-m.
s.rad.
040900/2
sub.
s-pyr.
D
s.l-m
070499/1
s.rad.
s.pyr

Fig. 2.

dal cell body layer (Sik et al., 1995), which was not the case for cells visualised in the present study. The cell bodies of the recorded cells were located primarily in the middle of stratum radiatum (Fig. 3C). The position of cell bodies appeared different from those of basket cells but this was probably a result of biased sampling. Somata were either round, ovoid or fusiform in shape, with the long axis often preferentially lying parallel to the strata (Figs. 1K, L and 2C, D), although this was not always the case. The soma gave rise to two to five primary dendrites that branched into secondary and tertiary dendrites close to the soma. The dendrites emerged in a radial pattern but then progressed almost exclusively in stratum radiatum, parallel to the strata boundaries (Fig. 2C, D). In some cases, the dendrites entered strata lacunosum-moleculare and oriens. The dendrites were often spiny, although occasionally aspiny dendrites could also be observed. The axon originated similarly to that of basket cells, branched many times in stratum radiatum, and also ramified almost exclusively within it (Fig. 2C, D). The axon often ran parallel to the boundaries of strata pyramidale and lacunosum-moleculare, covering the whole extent of the CA1 region and sometimes entering the subiculum (Fig. 2C, D). In two instances, a few axonal branches could also be observed entering stratum lacunosum-moleculare, approaching the fissure. In most cases, a few axonal branches also entered stratum pyramidale and, passing through it, branched in stratum oriens (e.g. Fig. 2D), where they usually reached the surface of the slice. Therefore, the extent of stratum oriens innervation is probably underrepresented in our sample.

Physiological properties of cholecystokinin-immunopositive interneurones

Passive and active membrane parameters were measured in order to determine if the cell types could be recognised on the basis of distinct physiological properties. Comparable sets of electrophysiological data were obtained in five basket and five Schaffer collateral-associated cells for analysis. The passive and active membrane properties of these 10 interneurones are summarised in Table 1, and determined from V_h close to −60 mV. Pro-CCK-immunopositive basket cells had a mean V_m of -61.40 ± 1.44 mV, mean R_N of 281.68 ± 35.66 MΩ, and mean τ_m of 25.07 ± 2.51 ms ($n = 5$). The passive membrane properties of the Schaffer collateral-associated cells were similar ($V_m = -60.60 \pm 3.14$ mV, $P > 0.05$; $R_N = 482.64 \pm 70.25$ MΩ, $P < 0.05$; $\tau_m = 26.12 \pm 3.13$ ms, $P > 0.05$, $n = 5$). These passive electrophysiological cell properties did not appear to vary with postnatal day, so that the properties of neurones recorded from P12 animals for both neurone groups were similar to those recorded from P17 animals (Table 1).

Application of large, hyperpolarising current steps at or close to V_m resulted in the appearance of a slowly activating, depolarising 'sag' potential in both basket and Schaffer collateral-associated cells (Fig. 4A_1, A_2, C_1, C_2), which in some cases was greater than 10 mV in amplitude. The 'sag' rectification ratio was calculated as 1.22 ± 0.06 for basket cells, and 1.51 ± 0.10 for Schaffer collateral-associated cells ($P < 0.05$, both $n = 5$). At the termination of the hyperpolarising current steps, depolarising rebound potentials were commonly elicited (mean amplitude 3.66 ± 1.19 mV in basket cells; 13.30 ± 3.02 mV in Schaffer collateral-associated cells, $P < 0.05$, both $n = 5$). In two Schaffer collateral-associated cells with V_h close to −60 mV, the depolarising rebound potentials were of sufficient amplitude to generate rebound action potentials (Fig. 4C_1). Such rebound action potential generation only occurred in the remaining Schaffer collateral-associated cells and in all basket cells following a shift of V_h close to action potential threshold.

Application of incrementing depolarising current steps at or close to V_m resulted in the generation of trains of tonically firing action potentials (Fig. 4A_1, C_1) whose frequency depended on the amplitude of the injected current step. The average action potential amplitude in basket cells was 76.92 ± 5.24 mV, with duration at half amplitude of 0.84 ± 0.05 ms, compared to 73.00 ± 4.82 mV ($P > 0.05$) and 1.06 ± 0.07 ms ($P < 0.05$) in Schaffer collateral-associated cells ($n = 5$) (Table 1). In all recorded neurones, individual action potentials initiated by small-amplitude depolarising current steps were followed by a clearly visible triphasic AHP ($n = 12$ cells) (Fig. 4A_3, C_3). This triphasic AHP consisted of an initial fAHP (mean amplitude 15.17 ± 1.53 mV in basket cells; 21.02 ± 2.59 mV in Schaffer collateral-associated cells, $P < 0.05$), followed by a mAHP (mean amplitude 5.20 ± 1.00 mV in basket cells; 3.18 ± 1.10 mV in Schaffer collateral-associated cells, $P > 0.05$), with these two AHPs separated by a small membrane recovery in the form of an ADP (mean amplitude 6.31 ± 2.02 mV in basket cells; 5.97 ± 1.32 mV in Schaffer collateral-associated cells, $P > 0.05$, both $n = 5$). Action potentials generated in response to larger depolarising currents steps, and therefore occurring at higher frequencies, partially obscured the triphasic AHP, although in some cases it was still clearly evident.

Action potentials could be generated at reasonably high frequencies in all recorded neurones in response to the largest (+375 pA) depolarising current step (40–100 Hz, $n = 10$) and showed little or no spike amplitude

Fig. 2. Axonal projection patterns of two pro-CCK-immunoreactive basket cells (A, P12 and B, P12) and two immunoreactive Schaffer collateral-associated cells (C, P16 and D, P16), also shown in Fig. 1. The basket cell axonal branches are concentrated in stratum pyramidale (s.pyr.) and they also innervate, to a smaller extent, the adjacent areas of strata radiatum (s.rad.) and oriens. In contrast, the axonal branches of Schaffer collateral-associated cells are mostly located in stratum radiatum; very few branches enter stratum pyramidale or pass through to stratum oriens, or enter stratum lacunosum-moleculare (s.l-m.). The dendritic trees of some cells (A–C) are severely truncated because most dendrites reached the surface of the slice. Numbers indicate cell identity of each recorded cell. Scale bars = 100 μm.

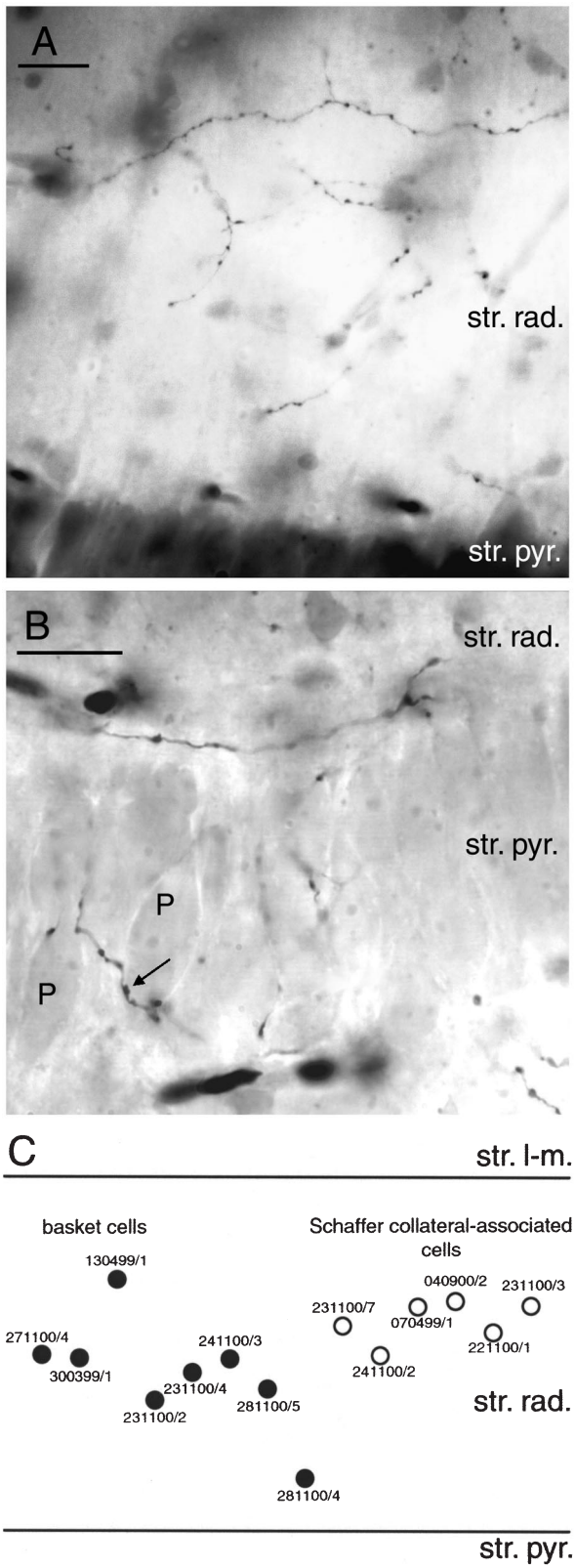

Fig. 3. (A, B) Light micrographs comparing the axon of a Schaffer collateral-associated cell (A, cell identity 070499/1, P16) in stratum radiatum (str.rad.), and that of a basket cell (B, cell identity 281100/4, P17) in stratum pyramidale (str.pyr.). Both cell types have axon collaterals densely studded with varicosities. Some boutons of the basket cell (e.g. arrow) surround pyramidal cell bodies (p). (C) Schematic diagram representing the normalised somatic position of basket (●) and Schaffer collateral-associated cells (○) in stratum radiatum relative to stratum pyramidale and stratum lacunosum-moleculare (str.l-m.). Numbers show the identity of each recorded cell. Scale bars = 20 μm.

attenuation (Fig. 4B$_1$, D$_1$). In both basket and Schaffer collateral-associated cells, the degree of spike frequency adaptation was pronounced in the first 200 ms of a spike train (Fig. 4B$_2$, D$_2$; early-phase adaptation ratio, basket cells = 1.72 ± 0.35; Schaffer collateral-associated cells = 1.99 ± 0.12, $P > 0.05$, both $n = 5$) but decreased thereafter (later-phase adaptation ratio, basket cell = 1.10 ± 0.02; Schaffer collateral-associated cell = 1.22 ± 0.02, $P < 0.05$, both $n = 5$). At the offset of large depolarising current steps in all recorded neurones, a large post-train AHP was typically generated, the amplitude of which was dependent on the size of the implemented current step, and the membrane potential only slowly returned to the initial holding potential (e.g. Fig. 4B$_1$).

Cholecystokinin- and calbindin-immunoreactive neurones in adult and developing hippocampus

The recorded neurones from developing hippocampi clearly show two distinct axonal patterns. However, many of the interneurone classes to which they were compared have only been described in adult animals. To test whether a transient expression of CCK during development might result in a difference in the distribution of immunopositive neurones, we compared hippocampal pro-CCK immunoreactivity in adult and developing animals. In agreement with previous studies (Greenwood et al., 1981; Somogyi et al., 1984; Harris et al., 1985; Hendry and Jones, 1985; Kosaka et al., 1985; Nunzi et al., 1985), pro-CCK-immunopositive cell bodies were present in all layers of the CA1 area of both adult and developing rat hippocampus (Fig. 5A, B). There was no obvious difference in position or density of immunoreactive cell bodies between the adult and developing rats. The immunoreactivity was present in perinuclear patches extending into the proximal dendrites in addition to a homogeneous weaker immunofluorescence signal throughout the cytoplasm. There were two distinct levels of somatic immunoreactivity. All pyramidal cells in stratum pyramidale showed weaker immunoreactivity than multipolar and spindle-shaped cells scattered throughout all layers (Fig. 5A, B). There was a higher density of immunopositive cells at the border of strata radiatum/lacunosum-moleculare in both the adult and developing rat.

One population of GABAergic interneurone that innervates the dendrites of pyramidal cells in strata radiatum and oriens expresses the Ca^{2+}-binding protein calbindin (Baimbridge and Miller, 1982; Baimbridge et al., 1991; Gulyás and Freund, 1996). Gulyás et al. (1991) showed that a few of these neurones express CCK as well in adult rats. Because we found the coexistence of pro-CCK and calbindin immunoreactivity in two of the recorded Schaffer collateral-associated interneurones, we tested further for the extent of coexistence in adult and

Table 1. Passive and active physiological properties of pro-CCK-immunopositive interneurones in stratum radiatum

Cell ID	Age	Resting membrane potential (mV)	Peak input resistance (MΩ)	Time constant (ms)	Action potential amplitude (mV)	Action potential duration (ms)	fAHP amplitude (mV)	Rectification ratio of 'sag'	Depolarising rebound potential (mV)
Basket									
231100/2	P12	−65	397.6	19.41	76.32	1.0	14.88	1.42	8.16
241100/3	P13	−63	316.2	31.62	74.47	0.8	14.88	1.14	3.33
271100/4	P16	−63	253.0	21.51	89.15	0.7	17.10	1.21	3.28
281100/4	P17	−58	185.0	22.21	59.07	0.9	19.10	1.25	2.39
281100/5	P17	−58	256.6	30.60	85.59	0.8	9.91	1.08	1.16
	P15 ± 1.05	−61.4 ± 1.44	281.68 ± 35.66	25.07 ± 2.51	76.92 ± 5.24	0.84 ± 0.05	15.17 ± 1.53	1.22 ± 0.05	3.66 ± 1.19
Schaffer collateral-associated									
310800/1	P12	−59	376.4	37.39	78.46	1.0	17.31	1.90	14.22
040900/2	P16	−66	607.4	27.72	89.67	0.8	23.92	1.45	20.45
231100/3	P12	−65	694.2	19.09	65.41	1.2	29.67	1.35	19.06
231100/7	P12	−49	385.4	23.48	65.75	1.2	18.85	1.34	5.36
241100/2	P13	−64	349.8	22.93	66.20	1.1	15.35	1.52	7.43
	P13.2 ± 0.73	−60.6 ± 3.14	482.64 ± 70.25*	26.12 ± 3.13	73.00 ± 4.82	1.06 ± 0.07*	21.02 ± 2.59*	1.51 ± 0.10*	13.30 ± 3.02*

Data are expressed as mean ± S.E.M. for each cell population. Significant differences indicated by * (Student's *t*-test, $P < 0.05$).

developing animals (Fig. 5C–F). Cells were counted in stratum radiatum and in the border region of strata radiatum and lacunosum, where both basket and Schaffer collateral-associated cells have been shown to have cell bodies (Hájos and Mody, 1997; Vida et al., 1998). Cells in the pyramidal cell layer were counted separately.

The frequencies of cells immunoreactive for one or both of the tested molecules were not different between animals (χ^2 test, $P > 0.05$) within each of the two age groups, therefore they were pooled (Table 2). Furthermore, there was no difference between the adult and the developing animals in the frequency of immunoreactive neurones (χ^2 test, $P > 0.05$), therefore they were pooled. In strata radiatum and lacunosum, in the evaluated cell population immunopositive for at least one molecule, on average, 56.0 ± 2.5% of cells were immunopositive only for pro-CCK, 20.7 ± 2.9% were immunopositive only for calbindin and 23.3 ± 2.3% were double-labelled (Fig. 5C, D). Of all the pro-CCK-positive cells, 29.2 ± 2.4% were also labelled for calbindin, whereas of all the calbindin-positive cells, 53.4 ± 5.3% were also pro-CCK-positive. The frequency of pro-CCK-positive cells which also expressed calbindin, or the proportion of calbindin-positive cells which also expressed pro-CCK, was not significantly different at the two tested ages ($P > 0.05$, χ^2 test).

In stratum pyramidale, interneurones were identified by their much stronger immunoreactivity for pro-CCK as compared to pyramidal cells, which were also immunopositive (Fig.- 5A, B). Few pro-CCK-positive interneurones were labelled for calbindin in the pyramidal layer of both the adult and the developing animals, and the proportion of double-labelled cells was not different, therefore they were pooled, giving an average of 17.1 ± 5.5% calbindin-labelled cells amongst pro-CCK-immunopositive putative interneurones. The calbindin-expressing, pro-CCK-immunonegative interneurones could not be counted in the pyramidal layer, because in the adult animal many pyramidal cells also express calbindin at a similar level to interneurones (Baimbridge and Miller, 1982; Baimbridge et al., 1991; Sloviter, 1989; Tóth and Freund, 1992). In the developing animals calbindin immunoreactivity was very weak in pyramidal cells.

We detected a significantly higher degree of coexistence of CCK and calbindin than reported previously using a different technique (Gulyás et al., 1991). Pyramidal cells express pro-CCK (Morino et al., 1994; see above) and a population of them also expresses calbindin (Baimbridge and Miller, 1982). Furthermore, pyramidal cells are scattered throughout stratum radiatum (Maccaferri and McBain, 1996b), and if these contained pro-CCK and/or calbindin immunoreactivity they would contribute to the population of immunoreactive cells counted. However, pro-CCK immunoreactivity is generally much weaker in pyramidal cells in stratum pyramidale, than in interneurones, and radiatum pyramidal cells have large apical dendrites (Maccaferri and McBain, 1996a,b; Gulyás et al., 1998). Therefore, we have scored weakly pro-CCK-immunoreactive cells in stratum radiatum as potential pyramidal cells on the basis of weak immunoreactivity and a major dendrite oriented towards stratum lacunosum-moleculare, before detecting the calbindin immunoreactivity. Overall, in six animals, only 7.1% ($n = 7$ cells) of pro-CCK-immunoreactive cells were scored as potential pyramidal cells in stratum radiatum, and 71.4% of them ($n = 5$ cells) were immunopositive for calbindin; but some or all of these cells could have been interneurones. Therefore, we conclude that, in our preparation, pyramidal cells made a minor if any contribution to pro-CCK- and calbindin-immunoreactive cell bodies in strata radiatum and lacunosum.

DISCUSSION

The main conclusions of this study are: (i) on the basis of axonal patterns, CCK-immunopositive interneurones in stratum radiatum can be identified as either basket or Schaffer collateral-associated cells; (ii) the tested physiological properties of the two types of CCK-immunopositive interneurones are only slightly different; (iii) for these two populations of cells, somatic location does

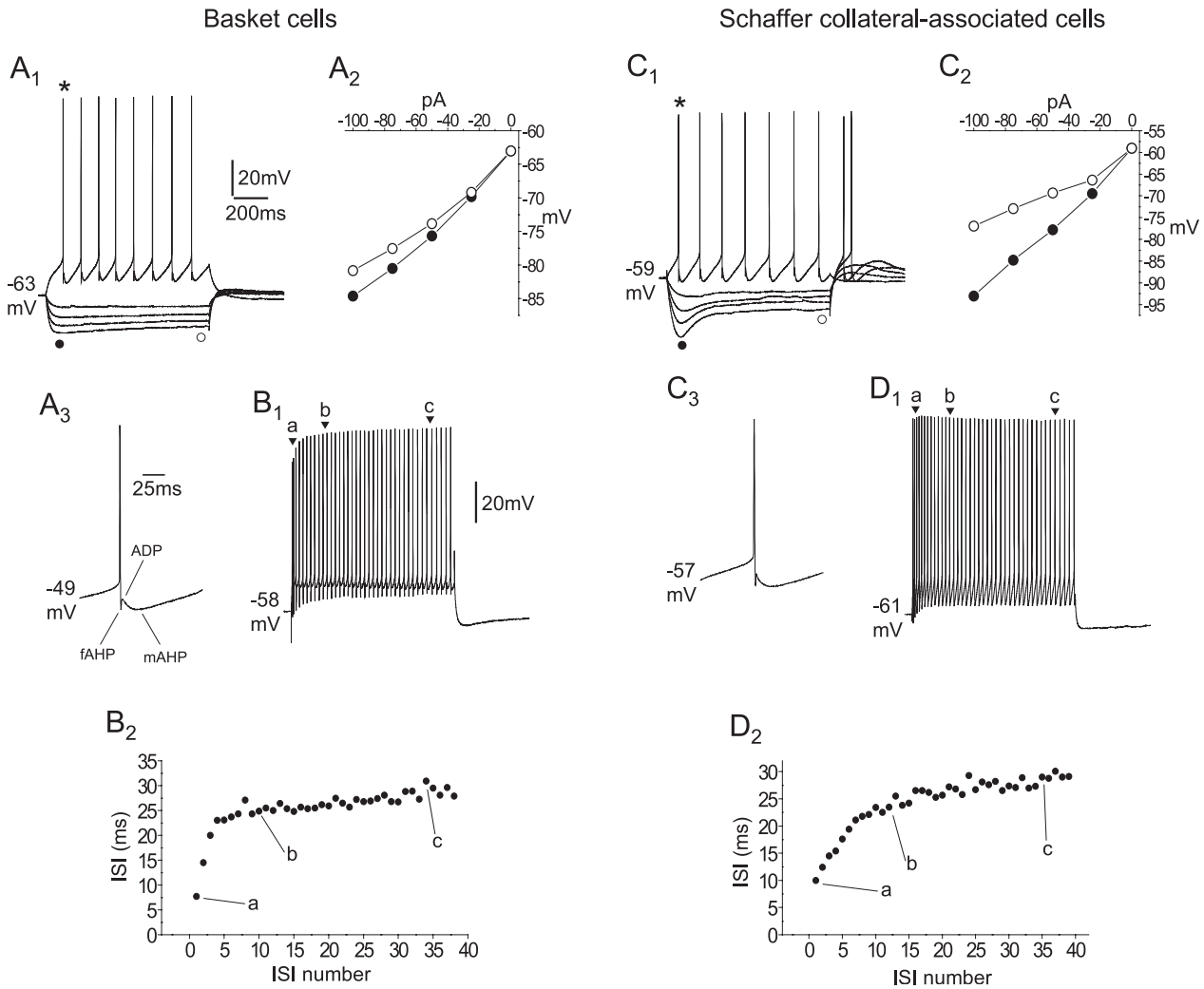

Fig. 4. Electrophysiological properties of pro-CCK-immunopositive interneurones. Comparison of the active membrane properties of two basket cells (A and B, cell identities 271100/4, P16, and 281100/4, P17, respectively) to two Schaffer collateral-associated cells (C and D, cell identities 310800/1, P12, and 040900/2, P16, respectively). (A_1, C_1) Voltage responses of a basket and Schaffer collateral-associated cell, to hyperpolarising (−100 to −25 pA) and a small depolarising (+50 and +25 pA, respectively) current steps. Voltage responses to hyperpolarising current steps in the Schaffer collateral-associated cell show a pronounced rectification, or 'sag', which is present to a lesser degree in the basket cell. Note how the depolarising rebound potentials at the step offset of the two largest voltage responses in the Schaffer collateral-associated cell are able to generate rebound action potentials. (A_2, C_2) Current–voltage plots of peak (●) and steady-state (○) hyperpolarising voltage responses as depicted in A_1 and C_1. (A_3, C_3) Expanded voltage traces (as marked by asterisks in A_1 and C_1, respectively) showing a single action potential and the characteristic triphasic after-hyperpolarisation following it. (B_1, D_1) Voltage responses of a basket and Schaffer collateral-associated cell to a large (+325 and +150 pA, respectively) depolarising current step. (B_2, D_2) Plot of the change in ISI against ISI number in the spike train for the voltage traces shown in B_1 and D_1. Letters (a, b) represent the points from which spike adaptation ratios were calculated relative to point c (see main text for details). Vertical calibration bar in A_1 also applies to A_3, C_1 and C_3. Horizontal calibration bar in A_1 also applies to B_1, C_1 and D_1. Horizontal calibration bar in A_3 also applies to C_3. Vertical calibration bar in B_1 also applies to D_1.

not appear to correlate with the cell type; (iv) at least some Schaffer collateral-associated cells probably express both CCK and calbindin; and (v) Schaffer collateral-associated cells are homologous to the double bouquet cells of the isocortex.

Identity of basket and Schaffer collateral-associated cells and homology to interneurones in the isocortex

Basket cells identified here as expressing pro-CCK are very likely identical to neurochemically uncharacterised basket cells described in stratum radiatum (Cossart et al., 2001a) and its border with stratum lacunosum (Kawaguchi and Hama, 1988; Vida et al., 1998). One CCK-immunopositive basket cell has been reported with cell body located in deep stratum oriens and having horizontal dendrites (Maccaferri et al., 2000). These basket cells are undoubtedly homologous to those in the isocortex, which have been shown to be immunopositive for CCK (Freund et al., 1986; Kawaguchi and Kubota, 1997, 1998; Kubota and Kawaguchi, 1997).

The Schaffer collateral-associated cells described here and elsewhere (Cossart et al., 2001a; Vida et al., 1998) in adult animals are very similar to 'radial trilaminar cells'

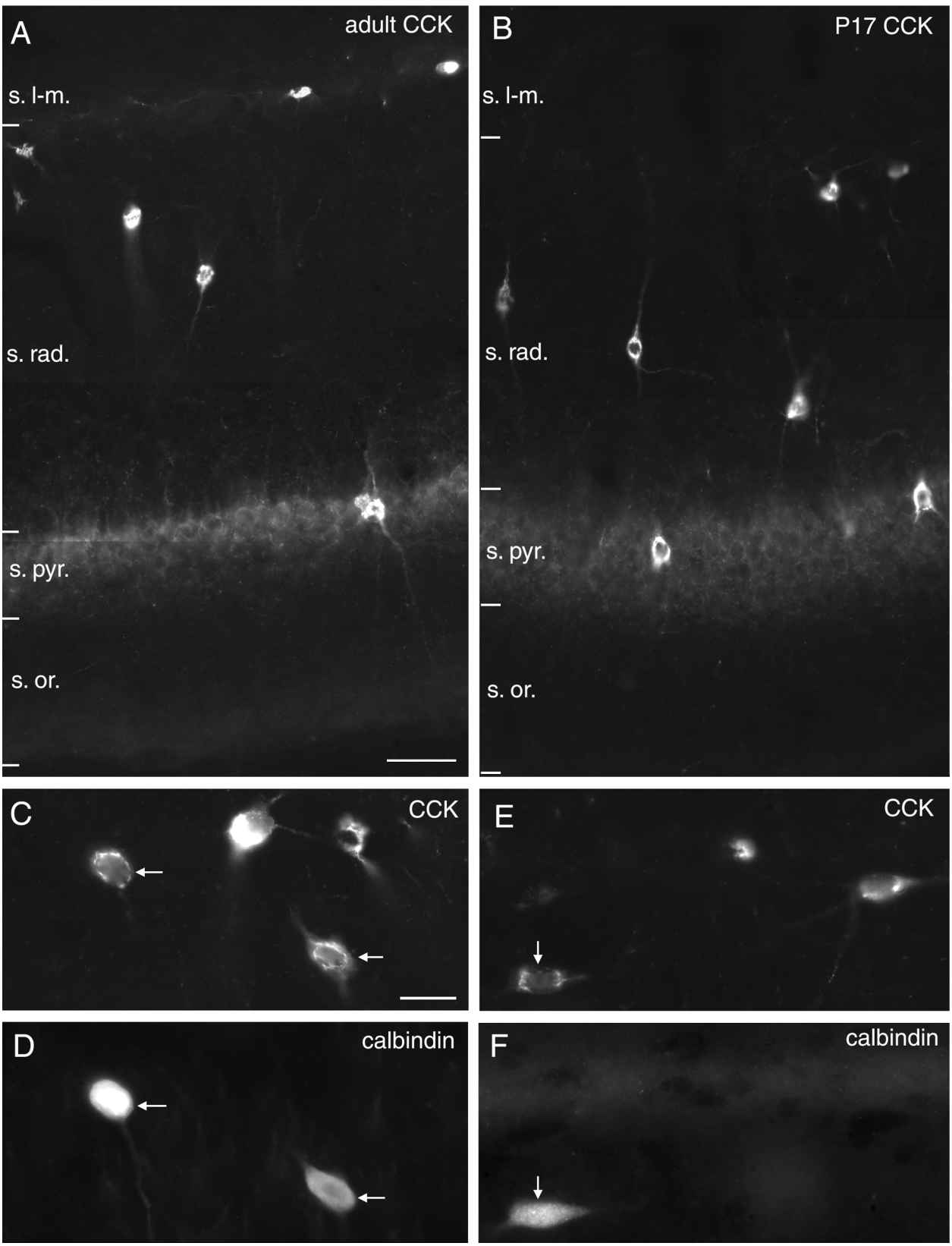

Fig. 5. (A, B) Fluorescence images showing a similar distribution of pro-CCK-immunoreactive neurones in the CA1 hippocampal area of an adult (A) and a P17 (B) animal. (C–F) Co-existence of pro-CCK (C, E, Alexa Fluor® 488 label) and calbindin (D, F, Cy™3 label) immunoreactivity in some interneurones (arrows) of stratum radiatum in adult (C, D) and P17 (E, F) animals. s.l-m., stratum lacunosum-moleculare; s.rad., stratum radiatum; s.pyr., stratum pyramidale; s.or., stratum oriens. Scale bars = 50 μm (A, B); 20 μm (C–F).

Table 2. Co-localisation of pro-CCK and calbindin (CB) immunoreactivity in interneurones of the CA1 area of adult and P17-P20 rats

Reference	Age	Area	Stratum radiatum and border area with lacunosum-moleculare								Stratum pyramidale	
			Total cells *n*	Only CCK+ %	Only CB+ %	CCK+ and CB+ %	Cells CCK+ *n*	also CB+ %	Cells CB+ *n*	also CCK+ %	Interneurones CCK+ *n*	also CB+ %
This study	Adult #1	CA1	83	55.4	12.0	32.5	73	37.0	37	73.0	25	12.0
	Adult #2		38	50.0	18.4	31.6	31	38.7	19	63.2	6	50.0
	Adult #3		30	50.0	30.0	20.0	21	28.6	15	40.0	14	7.1
	Adult #4		24	58.3	25.0	16.7	18	22.2	10	40.0	4	25.0
	Total adult		175				143		81		49	
	Mean ± S.E.M.			53.4 ± 4.1	21.4 ± 3.9	25.2 ± 4.0		31.6 ± 3.8		54.0 ± 8.3		23.5 ± 9.6
	P20 #1	CA1	41	63.4	9.8	26.8	37	29.7	15	73.3	14	7.1
	P20 #2		24	45.8	33.3	20.8	16	31.3	13	38.5	12	16.7
	P20 #3		22	59.1	18.2	22.7	18	27.8	9	55.6	5	0.0
	P17 #1		100	66.0	19.0	15.0	81	18.5	34	44.1	44	19.1
	Total P17–P20		187				152		71		75	
	Mean ± S.E.M.			58.6 ± 9.0	20.1 ± 4.9	21.3 ± 2.5		26.8 ± 2.9		52.9 ± 7.7		10.7 ± 4.4
	Total all ages		362				295		152		124	
	Mean ± S.E.M.			56.0 ± 2.5	20.7 ± 2.9	23.3 ± 2.3		29.2 ± 2.4		53.4 ± 5.3		17.1 ± 5.5
Gulyás et al., 1991	Adult	CA1	162	40.1	58.6	1.2	67	3.0	97	2.1	29	3.5
		CA3	164	31.7	59.8	8.5	66	21.2	112	12.5	6	0.0

described by Hájos and Mody (1997), and to various cells illustrated in the developing hippocampus (Morin et al., 1996; Parra et al., 1998; Banks et al., 2000). We prefer to use the term that signals the close association of the interneurone axon with the Schaffer collateral/commissural pathway termination zone. The expression of CCK by Schaffer collateral-associated cells makes it likely that they are homologous to the GABAergic double bouquet cells in the isocortex described in the cat and primates (Ramon y Cajal, 1899; Szentágothai, 1975; Somogyi and Cowey, 1981; Tamás et al., 1997). Double bouquet cells have been identified on the basis of tight radial axonal bundles and were shown to express CCK and calbindin (Freund et al., 1986; DeFelipe et al., 1989; DeFelipe and Jones, 1992; del Río and DeFelipe, 1997). The presence of both CCK and calbindin immunoreactivity in two Schaffer collateral-associated cells described here further supports the homology. The co-existence of CCK and calbindin immunoreactivity has also been described in the isocortex of the rat (Kubota and Kawaguchi, 1997). The characteristic tightly bundled axonal pattern of double bouquet cells was not seen in the hippocampus, but this is likely to be due to the different organisation of the dendrites of the target cell population. In the isocortex double bouquet cells innervate a radially oriented column of cells in layers 4–6, whereas in the hippocampus the target cell population is spread out tangentially. In supragranular layers 2 and 3 of the isocortex, the portion of double bouquet cell axon, which targets a more laterally distributed postsynaptic cell population, is more similar to the axon of Schaffer collateral-associated cells.

A hallmark of double bouquet cells is that they only give synapses to dendritic shafts and spines and ignore somata even when the axon runs in direct membrane apposition to soma (Somogyi and Cowey, 1981; Freund et al., 1986; DeFelipe et al., 1989; Tamás et al., 1997). In particular, Tamás et al. (1997) studied a large sample of postsynaptic targets from a homogeneous population of double bouquet cells and also showed on a simultaneously recorded pyramidal cell that spines were the main synaptic target. In the hippocampus, a previous study reported that Schaffer collateral-associated cells make synapses with small-calibre side branches of the pyramidal cell apical dendrite, and aspiny dendritic shafts of presumed interneurones (Vida et al., 1998), but never, or only rarely, with spines. Therefore, these GABAergic neurones in the isocortex and hippocampus differ in the innervation of spines, but the shafts of small dendritic branches are a common postsynaptic element in the two cortical areas. In addition, CCK-positive terminals have been observed to target distal dendritic sites of pyramidal cells and GABAergic cells (Harris et al., 1985; Hendry and Jones, 1985; Nunzi et al., 1985). Similarly, calbindin-positive terminals have been identified as targeting distal dendritic sites of pyramidal cells and GABAergic cells in stratum radiatum (Gulyás and Freund, 1996). Therefore, it appears that Schaffer collateral-associated cells mostly target dendritic shafts of pyramidal cells and other GABAergic cells; the latter may constitute other CCK-expressing cells, as they have been shown to be

interconnected in stratum radiatum (Harris et al., 1985; Nunzi et al., 1985).

Intrinsic physiological properties

Many of both the passive and active intrinsic membrane properties of CCK-expressing basket and Schaffer collateral-associated cells were not significantly different. A somewhat larger R_N in Schaffer collateral-associated compared to basket cells was the only significant difference in passive membrane properties, and the values were similar to those observed in other CA1 interneurones, as were the V_m and τ_m (Williams et al., 1994; Morin et al., 1996; Parra et al., 1998). Some active membrane properties, such as the action potential duration and fAHP amplitude, were significantly different in the two groups. Values for both cell groups were in the range observed in previous patch and sharp microelectrode studies (Lacaille et al., 1987; Lacaille and Schwartzkroin, 1988; Buhl et al., 1994b, 1996; Williams et al., 1994; Zhang and McBain, 1995; Morin et al., 1996; Ali et al., 1998; Ali and Thomson, 1998; Vida et al., 1998).

Triphasic AHPs, similar to those found here, have been recorded previously in hippocampal interneurones (Williams et al., 1994; Zhang and McBain, 1995; Morin et al., 1996). In two of these studies (Williams et al., 1994; Morin et al., 1996) the triphasic AHPs have been recorded in interneurones located at the strata radiatum/lacunosum border. It is possible that some of the cells were CCK-positive basket and Schaffer collateral-associated cells as described here. In several neuronal cell types, the fAHP component probably arises due to the activation of voltage-dependent K^+ channels (Storm, 1987; Baranyi et al., 1993; Zhang and McBain, 1995; Bevan and Wilson, 1999), whilst the mAHP component is mediated by Ca^{2+}-activated K^+ channels (Storm, 1989; Williamson and Alger, 1990; Zhang and McBain, 1995; Bevan and Wilson, 1999; Aoki and Baraban, 2000; Savic et al., 2001). In addition, Pawelzik et al. (2000) suggested that the waveform of the triphasic AHP recorded in CA1 basket cells close to stratum pyramidale is sculpted by the autaptic activation of $GABA_A$ receptors. Given that the dendritic arborisation and axonal distribution of both CCK-expressing basket and Schaffer collateral-associated cells overlap, autaptic GABAergic responses may contribute to the waveform of the triphasic AHPs. However, this mechanism does not account for virtually identical triphasic AHPs recorded in CCK-expressing cells with clear truncation of the axon close to its origin, before any boutons were emitted.

The 'sag' rectification ratio and depolarising rebound potential were somewhat larger in Schaffer collateral-associated compared to the basket cells. In numerous cell types both the 'sag' potential and depolarising rebound potentials have been shown to be caused by the activation and then slow deactivation of the hyperpolarisation-activated cation current, I_h, during and following the termination of phases of hyperpolarisation, respectively (Maccaferri et al., 1993; Solomon and Nerbonne, 1993; Womble and Moises, 1993; Bayliss et al., 1994; Maccaferri and McBain, 1996a,b; Pape, 1996; Savic et al., 2001). In addition, the activation of low-threshold Ca^{2+} channels (Fraser and MacVicar, 1991) may also contribute to the depolarising rebound potentials, but we have not explored these mechanisms. Both basket and Schaffer collateral-associated cells showed pronounced spike frequency adaptation at the onset of high-frequency spike trains, which gradually diminished throughout the duration of that train. This pattern suggests that in both cell types, short-duration inputs elicit a burst of fast action potentials, whereas more prolonged inputs will be relatively rapidly adapted. The potentially numerous mechanisms underlying spike frequency adaptation in these cell types remain to be explored.

Functional implications

Basket cells (Buhl et al., 1994a; Cobb et al., 1995; Miles et al., 1996; Vida et al., 1998; Ali et al., 1999; Pawelzik et al., 1999; Maccaferri et al., 2000; Thomson et al., 2000) and Schaffer collateral-associated cells (Vida et al., 1998) evoke $GABA_A$ receptor-mediated fast inhibitory postsynaptic potentials (IPSPs) in their target neurones. However, due to the different subcellular domain preference for their efferent synapses, they probably subserve different functions. Basket cells have been identified as playing a role in the phasing of pyramidal cell firing (Cobb et al., 1995; Miles et al., 1996). The wide arborisation of basket cell dendrites throughout all layers of the CA1 suggests that they may do this in response to a variety of excitatory inputs. In addition to CCK-expressing basket cells, another population that expresses PV also targets pyramidal cell somata and proximal dendrites. Although the terminals of the two distinct basket cell populations are intermingled on the postsynaptic cell surface, they act through partially distinct $GABA_A$ receptors (Thomson et al., 2000). The synapses made by terminals of CCK-expressing basket cells, which comprise about one third of the synapses on the soma, contain a much higher level of $\alpha 2$ subunit-containing receptors than those made by PV-positive terminals, although the two populations contain a similar number of receptors (Nyíri et al., 2001).

Interneurone populations that target the distal dendrites of neurones have been suggested to subserve a variety of different roles, including control of Ca^{2+} electrogenesis in the dendrites and shunting of incoming excitatory inputs (Miles et al., 1996; Tsubokawa and Ross, 1996), or the rescaling of excitatory postsynaptic potentials (EPSPs) (Halasy and Somogyi, 1993). The fact that Schaffer collateral-associated cell somata and dendrites are primarily aligned with the Schaffer collateral/commissural input (Hájos and Mody, 1997; Vida et al., 1998; Gulyás et al., 1999) implies that they may monitor the flow of activity from the CA3 region and provide feed-forward inhibition to the small dendrites of CA1 pyramidal cells (McBain and Fisahn, 2001). The dendritic IPSPs could also co-operate with voltage-sensitive ion channels and dendritic oscillations in regulating the timing of EPSPs, rather than antagonising input from the CA3 region. Recent recordings from stratum radia-

tum interneurones showed that EPSPs evoked by Schaffer collateral/commissural pathway stimulation lead to reliable and precisely timed action potentials in these cells (Fricker and Miles, 2000). The interneurones probably included similar cells to those presented here, therefore it is likely that both basket and Schaffer collateral-associated cells will be activated together under certain circumstances. However, potential differences in interactions at the target sites of their efferent synapses, on the somata and in the dendrites, respectively, together with possible differences in the short-term plasticity of the synapses, might lead to differential effects and redistribution of GABAergic input on the postsynaptic pyramidal cell. In addition, Schaffer collateral-associated cells may serve to synchronise populations of GABAergic interneurones in the CA1 region due to the likelihood that Schaffer collateral-associated cells also target these cells.

Synaptically released CCK may have numerous roles in the hippocampus, and in addition to GABAergic neurones, pyramidal cells also express CCK (Morino et al., 1994), therefore multiple sources and mechanisms may be involved. Direct postsynaptic excitation of hippocampal pyramidal neurones has been observed following CCK application. The mechanisms have been suggested as: (i) activation of a non-selective cation current (Dodd and Kelly, 1981); (ii) modulation of transient voltage-dependent K^+ currents (Buckett and Saint, 1989; Saint and Buckett, 1991); (iii) suppression of 'leak' voltage-independent K^+ current (Boden and Hill, 1988; Buckett and Saint, 1989; Shinohara and Kawasaki, 1997); and (iv) suppression of Ca^{2+}-activated K^+ current (Shinohara and Kawasaki, 1997). CCK also has a directly excitatory effect on interneurones in stratum radiatum, causing depolarisation through a reduction in a resting K^+ current (Miller et al., 1997). This subsequently causes an increase in $GABA_A$ receptor-mediated inhibition in pyramidal neurones (MacVicar et al., 1987; Miller and Lupica, 1994; Miller et al., 1997), although a reduction has also been observed (Jaffe et al., 1987). Thus, CCK-releasing, GABAergic interneurones may cause concomitant postsynaptic inhibition and excitation, provided enough CCK is released to influence the outcome. Perhaps the most interesting role of CCK in the cerebral cortex is its ability to facilitate the release of GABA in slices of neocortex and hippocampus (Sheehan and de Belleroche, 1983; Pérez de la Mora et al., 1993), although not from isolated, hippocampal synaptosomes (Breukel et al., 1997). The elucidation of the functional role of CCK in the hippocampus would be further enhanced if the precise subcellular location of CCK receptors were known. The CNS predominantly expresses the B-type (CCK-B) rather than the A-type receptor (Böhme et al., 1988; Woodruff et al., 1991; Pérez de la Mora et al., 1993; Wank, 1995; Miller et al., 1997; Shinohara and Kawasaki, 1997). Given the widespread somato-dendritic distribution of CCK-positive terminals on pyramidal neurones and interneurones (Harris et al., 1985; Hendry and Jones, 1985; Nunzi et al., 1985), CCK-B receptors are presumably similarly distributed over the entire cellular axis of pyramidal cells as well as both CCK-expressing and non-CCK-expressing interneurone populations. The possibility also exists that CCK-B receptors are present on presynaptic terminals and influence transmitter release through a feed-back mechanism, as described for a variety of other neurone types (Léna et al., 1997; Saleh et al., 1997; Parker, 2000).

CCK-immunopositive, GABAergic interneurones in the hippocampus and isocortex have been shown to express a high level of the cannabinoid type 1 (CB1) receptor (Marsicano and Lutz, 1999; Tsou et al., 1999). The receptor is located presynaptically on basket cell terminals and probably also on terminals of CCK-positive cells which target the dendrites (Katona et al., 1999; Hájos et al., 2000; Katona et al., 2000), thus the two cell types described here share several signalling mechanisms. Activation of CB1 receptors inhibits the release of GABA from CCK-expressing interneurones in the hippocampal formation (Katona et al., 1999, 2000; Hoffman and Lupica, 2000; Irving et al., 2000). This down-regulation of GABA release by endogenous CB1 agonists has been implicated in depolarisation-induced suppression of inhibition, long-term potentiation, modulation of network oscillations and higher cognitive processes involving the hippocampus (Howlett, 1995; Stella et al., 1997; Hájos et al., 2000; Ohno-Shosaku et al., 2001; Wilson and Nicoll, 2001). In addition, the 5-hydroxytryptamine type 3 receptor is expressed at a high level in GABAergic, CCK-positive interneurones (Tecott et al., 1993; Morales et al., 1996; Morales and Bloom, 1997), but it remains to be established if both cell types described in the present study express it at similar levels.

CONCLUSION

Schaffer collateral-associated cells represent a novel CCK-expressing interneurone population in the hippocampal CA1 region. Some of them also express calbindin. They are homologous to the double bouquet cells found in the isocortex, which are also CCK- and calbindin-immunopositive. The unique layout of the hippocampus has made obvious that GABAergic terminals of Schaffer collateral-associated cells are co-aligned with a specific glutamatergic pathway, the Schaffer collateral/commissural input to CA1 pyramidal cells. In the isocortex the excitatory partner of double bouquet cells is not known, if indeed such a specific partner exists. The functional role of the Schaffer collateral-associated cell population is as yet undetermined, although they are likely to modulate, in a feed-forward manner, the Schaffer collateral/commissural input to the CA1 region.

Acknowledgements—The authors are grateful to Dr Andrea Varro for the gift of antibodies to pro-CCK. Drs Francesco Ferraguti, Yannis Dalezios and Marco Capogna provided helpful comments on a previous version of the manuscript.

REFERENCES

Acsády, L., Görcs, T.J., Freund, T.F., 1996. Different populations of vasoactive intestinal polypeptide-immunoreactive interneurons are specialized to control pyramidal cells or interneurons in the hippocampus. Neuroscience 73, 317–334.

Acsády, L., Katona, I., Martínez-Guijarro, F.J., Buzsáki, G., Freund, T.F., 2000. Unusual target selectivity of perisomatic inhibitory cells in the hilar region of the rat hippocampus. J. Neurosci. 20, 6907–6919.

Ali, A.B., Bannister, A.P., Thomson, A.M., 1999. IPSPs elicited in CA1 pyramidal cells by putative basket cells in slices of adult rat hippocampus. Eur. J. Neurosci. 11, 1741–1753.

Ali, A.B., Deuchars, J., Pawelzik, H., Thomson, A.M., 1998. CA1 pyramidal to basket and bistratified cell EPSPs: dual intracellular recordings in rat hippocampal slices. J. Physiol. 507, 201–217.

Ali, A.B., Thomson, A.M., 1998. Facilitating pyramid to horizontal oriens-alveus interneurone inputs: dual intracellular recordings in slices of rat hippocampus. J. Physiol. 507, 185–199.

Aoki, T., Baraban, S.C., 2000. Properties of a calcium-activated K^+ current on interneurons in the developing rat hippocampus. J. Neurophysiol. 83, 3453–3461.

Baimbridge, K.G., Miller, J.J., 1982. Immunohistochemical localization of calcium-binding protein in the cerebellum, hippocampal formation and olfactory bulb of the rat. Brain Res. 245, 223–229.

Baimbridge, K.G., Peet, M.J., McLennan, H., Church, J., 1991. Bursting response to current-evoked depolarization in rat CA1 pyramidal neurons is correlated with lucifer yellow dye coupling but not with the presence of calbindin-D_{28k}. Synapse 7, 269–277.

Banks, M.I., White, J.A., Pearce, R.A., 2000. Interactions between distinct $GABA_A$ circuits in hippocampus. Neuron 25, 449–457.

Baranyi, A., Szente, M.B., Woody, C.D., 1993. Electrophysiological characterization of different types of neurons recorded *in vivo* in the motor cortex of the cat. II. Membrane parameters, action potentials, current-induced voltage responses and electrotonic structures. J. Neurophysiol. 69, 1865–1879.

Bayliss, D.A., Viana, F., Bellingham, M.C., Berger, A.J., 1994. Characteristics and postnatal development of a hyperpolarization-activated inward current in rat hypoglossal motoneurons *in vitro*. J. Neurophysiol. 71, 119–128.

Bevan, M.D., Wilson, C.J., 1999. Mechanisms underlying spontaneous oscillation and rhythmic firing in rat subthalamic neurons. J. Neurosci. 19, 7617–7628.

Boden, P.R., Hill, R.G., 1988. Effects of cholecystokinin and pentagastrin on rat hippocampal neurones maintained *in vitro*. Neuropeptides 12, 95–103.

Böhme, G.A., Stutzmann, J.-M., Blanchard, J.-C., 1988. Excitatory effects of cholecystokinin in rat hippocampus: pharmacological response compatible with 'central'- or B-type CCK receptors. Brain Res. 451, 309–318.

Breukel, A.I.M., Lopes da Silva, F.H., Ghijsen, W.E.J.M., 1997. Cholecystokinin (CCK-8) modulates vesicular release of excitatory amino acids in rat hippocampal nerve endings. Neurosci. Lett. 234, 67–70.

Buckett, K.J., Saint, D.A., 1989. Cholecystokinin modulates voltage dependent K^+ currents in cultured rat hippocampal neurones. Neurosci. Lett. 107, 162–166.

Buhl, E.H., Halasy, K., Somogyi, P., 1994a. Diverse sources of hippocampal unitary inhibitory postsynaptic potentials and the number of synaptic release sites. Nature 368, 823–828.

Buhl, E.H., Han, Z.-S., Lörinczi, Z., Stezhka, V.V., Karnup, S.V., Somogyi, P., 1994b. Physiological properties of anatomically identified axo-axonic cells in the rat hippocampus. J. Neurophysiol. 71, 1289–1307.

Buhl, E.H., Szilágyi, T., Halasy, K., Somogyi, P., 1996. Physiological properties of anatomically identified basket and bistratified cells in the CA1 area of the rat hippocampus *in vitro*. Hippocampus 6, 294–305.

Cobb, S.R., Buhl, E.H., Halasy, K., Paulsen, O., Somogyi, P., 1995. Synchronization of neuronal activity in hippocampus by individual GABAergic interneurons. Nature 378, 75–78.

Cossart, R., Dinocourt, C., Hirsch, J.C., Merchan-Perez, A., De Felipe, J., Ben-Ari, Y., Esclapez, M., Bernard, C., 2001a. Dendritic but not somatic GABAergic inhibition is decreased in experimental epilepsy. Nature Neurosci. 4, 52–62.

Cossart, R., Tyzio, R., Dinocourt, C., Esclapez, M., Hirsch, J.C., Ben-Ari, Y., Bernard, C., 2001b. Presynaptic kainate receptors that enhance the release of GABA on CA1 hippocampal interneurons. Neuron 29, 497–508.

DeFelipe, J., Hendry, S.H.C., Jones, E.G., 1989. Synapses of double bouquet cells in monkey cerebral cortex visualized by calbindin immunoreactivity. Brain Res. 503, 49–54.

DeFelipe, J., Jones, E.G., 1992. High-resolution light and electron microscopic immunocytochemistry of colocalized GABA and calbindin D-28k in somata and double bouquet cell axons of monkey somatosensory cortex. Eur. J. Neurosci. 4, 46–60.

del Río, M.R., DeFelipe, J., 1997. Double bouquet cell axons in the human temporal neocortex: relationship to bundles of myelinated axons and colocalization of calretinin and calbindin D-28k immunoreactivities. J. Chem. Neuroanat. 13, 243–251.

Dodd, J., Kelly, J.S., 1981. The actions of cholecystokinin and related peptides on pyramidal neurones of the mammalian hippocampus. Brain Res. 205, 337–350.

Fraser, D.D., MacVicar, B.A., 1991. Low-threshold transient calcium current in rat hippocampal lacunosum-moleculare interneurons: kinetics and modulation by neurotransmitters. J. Neurosci. 11, 2812–2820.

Freund, T.F., Buzsáki, G., 1996. Interneurons of the hippocampus. Hippocampus 6, 347–470.

Freund, T.F., Maglóczky, Zs., Soltész, I., Somogyi, P., 1986. Synaptic connections, axonal and dendritic patterns of neurons immunoreactive for cholecystokinin in the visual cortex of the cat. Neuroscience 19, 1133–1159.

Fricker, D., Miles, R., 2000. EPSP amplification and the precision of spike timing in hippocampal neurons. Neuron 28, 559–569.

Greenwood, R.S., Godar, E.S., Reaves, T.A., Jr., Hayward, J.N., 1981. Cholecystokinin in hippocampal pathways. J. Comp. Neurol. 203, 335–350.

Gulyás, A.I., Freund, T.F., 1996. Pyramidal cell dendrites are the primary targets of calbindin D28k-immunoreactive interneurons in the hippocampus. Hippocampus 6, 525–534.

Gulyás, A.I., Hájos, N., Freund, T.F., 1996. Interneurons containing calretinin are specialized to control other interneurons in the rat hippocampus. J. Neurosci. 16, 3397–3411.

Gulyás, A.I., Megías, M., Emri, Zs., Freund, T.F., 1999. Total number and ratio of excitatory and inhibitory synapses converging onto single interneurons of different types in the CA1 area of the rat hippocampus. J. Neurosci. 19, 10082–10097.

Gulyás, A.I., Miles, R., Hájos, N., Freund, T.F., 1993. Precision and variability in postsynaptic target selection of inhibitory cells in the hippocampal CA3 region. Eur. J. Neurosci. 5, 1729–1751.

Gulyás, A.I., Tóth, K., Dános, P., Freund, T.F., 1991. Subpopulations of GABAergic neurons containing parvalbumin, calbindin D28k and cholecystokinin in the rat hippocampus. J. Comp. Neurol. 312, 371–378.

Gulyás, A.I., Tóth, K., McBain, C.J., Freund, T.F., 1998. Stratum radiatum giant cells: a type of principal cell in the rat hippocampus. Eur. J. Neurosci. 10, 3813–3822.
Hájos, N., Katona, I., Naiem, S.S., Mackie, K., Ledent, C., Mody, I., Freund, T.F., 2000. Cannabinoids inhibit hippocampal GABAergic transmission and network oscillations. Eur. J. Neurosci. 12, 3239–3249.
Hájos, N., Mody, I., 1997. Synaptic communication among hippocampal interneurons: properties of spontaneous IPSCs in morphologically identified cells. J. Neurosci. 17, 8427–8442.
Halasy, K., Somogyi, P., 1993. Subdivisions in the multiple GABAergic innervation of granule cells in the dentate gyrus of the rat hippocampus. Eur. J. Neurosci. 5, 411–429.
Han, Z.-S., Buhl, E.H., Lörinczi, Z., Somogyi, P., 1993. A high degree of spatial selectivity in the axonal and dendritic domains of physiologically identified local-circuit neurons in the dentate gyrus of the rat hippocampus. Eur. J. Neurosci. 5, 395–410.
Harris, K.M., Marshall, P.E., Landis, D.M.D., 1985. Ultrastructural study of cholecystokinin-immunoreactive cells and processes in area CA1 of the rat hippocampus. J. Comp. Neurol. 233, 147–158.
Hendry, S.H.C., Jones, E.G., 1985. Morphology of synapses formed by cholecystokinin-immunoreactive axon terminals in regio superior of rat hippocampus. Neuroscience 16, 57–68.
Hoffman, A.F., Lupica, C.R., 2000. Mechanisms of cannabinoid inhibition of $GABA_A$ synaptic transmission in the hippocampus. J. Neurosci. 20, 2470–2479.
Howlett, A.C., 1995. Pharmacology of cannabinoid receptors. Annu. Rev. Pharmacol. Toxicol. 35, 607–634.
Irving, A.J., Coutts, A.A., Harvey, J., Rae, M.G., Mackie, K., Bewick, G.S., Pertwee, R.G., 2000. Functional expression of cell surface cannabinoid CB_1 receptors on presynaptic inhibitory terminals in cultured rat hippocampal neurons. Neuroscience 98, 253–262.
Jaffe, D.B., Aitken, P.G., Nadler, J.V., 1987. The effects of cholecystokinin and cholecystokinin antagonists on synaptic function in the CA1 region of the rat hippocampal slice. Brain Res. 415, 197–203.
Katona, I., Sperlágh, B., Maglóczky, Z., Sántha, E., Köfalvi, A., Czirják, S., Mackie, K., Vizi, E.S., Freund, T.F., 2000. GABAergic interneurons are the targets of cannabinoid actions in the human hippocampus. Neuroscience 100, 797–804.
Katona, I., Sperlágh, B., Sík, A., Käfalvi, A., Vizi, E.S., Mackie, K., Freund, T.F., 1999. Presynaptically located CB1 cannabinoid receptors regulate GABA release from axon terminals of specific hippocampal interneurons. J. Neurosci. 19, 4544–4558.
Katsumaru, H., Kosaka, T., Heizmann, C.W., Hama, K., 1988. Immunocytochemical study of GABAergic neurons containing the calcium-binding protein parvalbumin in the rat hippocampus. Exp. Brain Res. 72, 347–362.
Kawaguchi, Y., Hama, K., 1987. Two subtypes of non-pyramidal cells in rat hippocampal formation identified by intracellular recording and HRP injection. Brain Res. 411, 190–195.
Kawaguchi, Y., Hama, K., 1988. Physiological heterogeneity of nonpyramidal cells in rat hippocampal CA1 region. Exp. Brain Res. 72, 494–502.
Kawaguchi, Y., Katsumaru, H., Kosaka, T., Heizmann, C.W., Hama, K., 1987. Fast spiking cells in rat hippocampus (CA_1 region) contain the calcium-binding protein parvalbumin. Brain Res. 416, 369–374.
Kawaguchi, Y., Kubota, Y., 1997. GABAergic cell subtypes and their synaptic connections in rat frontal cortex. Cerebr. Cortex 7, 476–486.
Kawaguchi, Y., Kubota, Y., 1998. Neurochemical features and synaptic connections of large physiologically-identified GABAergic cells in the rat frontal cortex. Neuroscience 85, 677–701.
Kosaka, T., Katsumaru, H., Hama, K., Wu, J.-Y., Heizmann, C.W., 1987. GABAergic neurons containing the Ca^{2+}-binding protein parvalbumin in the rat hippocampus and dentate gyrus. Brain Res. 419, 119–130.
Kosaka, T., Kosaka, K., Tateishi, K., Hamaoka, Y., Yanaihara, N., Wu, J.-Y., Hama, K., 1985. GABAergic neurons containing CCK-8-like and/or VIP-like immunoreactivities in the rat hippocampus and dentate gyrus. J. Comp. Neurol. 239, 420–430.
Kubota, Y., Kawaguchi, Y., 1997. Two distinct subgroups of cholecystokinin-immunoreactive cortical interneurons. Brain Res. 752, 175–183.
Lacaille, J.-C., Mueller, A.L., Kunkel, D.D., Schwartzkroin, P.A., 1987. Local circuit interactions between oriens/alveus interneurons and CA1 pyramidal cells in hippocampal slices: electrophysiology and morphology. J. Neurosci. 7, 1979–1993.
Lacaille, J.-C., Schwartzkroin, P.A., 1988. Stratum lacunosum-moleculare interneurons of hippocampal CA1 region. I. Intracellular response characteristics, synaptic responses, and morphology. J. Neurosci. 8, 1400–1410.
Léna, I., Roques, B.P., Durieux, C., 1997. Dual modulation of dopamine release from anterior nucleus accumbens through cholecystokinin-B receptor subsites. J. Neurochem. 68, 162–168.
Maccaferri, G., Mangoni, M., Lazzari, A., DiFrancesco, D., 1993. Properties of the hyperpolarization-activated current in rat hippocampal CA1 pyramidal cells. J. Neurophysiol. 69, 2129–2136.
Maccaferri, G., McBain, C.J., 1996a. The hyperpolarization-activated current (I_h) and its contribution to pacemaker activity in rat CA1 hippocampal stratum oriens-alveus interneurones. J. Physiol. 497, 119–130.
Maccaferri, G., McBain, C.J., 1996b. Long-term potentiation in distinct subtypes of hippocampal nonpyramidal neurons. J. Neurosci. 16, 5334–5343.
Maccaferri, G., Roberts, J.D.B., Szucs, P., Cottingham, C.A., Somogyi, P., 2000. Cell surface domain specific postsynaptic currents evoked by identified GABAergic neurones in rat hippocampus *in vitro*. J. Physiol. 524, 91–116.
MacVicar, B.A., Kerrin, J.P., Davison, J.S., 1987. Inhibition of synaptic transmission in the hippocampus by cholecystokinin (CCK) and its antagonism by a CCK analog (CCK_{27-33}). Brain Res. 406, 130–135.
Magistretti, J., Mantegazza, M., Guatteo, E., Wanke, E., 1996. Action potentials recorded with patch-clamp amplifiers: are they genuine? Trends Neurosci. 19, 530–534.
Marsicano, G., Lutz, B., 1999. Expression of the cannabinoid receptor CB1 in distinct neuronal subpopulations in the adult mouse forebrain. Eur. J. Neurosci. 11, 4213–4225.
McBain, C.J., Fisahn, A., 2001. Interneurons unbound. Nat. Rev. 2, 11–24.
Miles, R., Tóth, K., Gulyás, A.I., Hájos, N., Freund, T.F., 1996. Differences between somatic and dendritic inhibition in the hippocampus. Neuron 16, 815–823.
Miller, K.K., Hoffer, A., Svoboda, K.R., Lupica, C.R., 1997. Cholecystokinin increases GABA release by inhibiting a resting K^+ conductance in hippocampal interneurons. J. Neurosci. 17, 4994–5003.
Miller, K.K., Lupica, C.R., 1994. Morphine-induced excitation of pyramidal neurons is inhibited by cholecystokinin in the CA1 region of the rat hippocampal slice. J. Pharmacol. Exp. Ther. 268, 753–761.
Morales, M., Battenberg, E., de Lecea, L., Bloom, F.E., 1996. The type 3 serotonin receptor is expressed in a subpopulation of GABAergic neurons in the rat neocortex and hippocampus. Brain Res. 731, 199–202.
Morales, M., Bloom, F.E., 1997. The 5-HT_3 receptor is present in different subpopulations of GABAergic neurons in the rat telencephalon. J. Neurosci. 17, 3157–3167.
Morin, F., Beaulieu, C., Lacaille, J.-C., 1996. Membrane properties and synaptic currents evoked in CA1 interneuron subtypes in rat hippocampal slices. J. Neurophysiol. 76, 1–16.

Morino, P., Herrara-Marschitz, M., Castel, M.N., Ungerstedt, U., Varro, A., Dockray, G., Hökfelt, T., 1994. Cholecystokinin in cortico-striatal neurons in the rat: immunohistochemical studies at the light and electron microscopical level. Eur. J. Neurosci. 6, 681–692.
Nomura, T., Fukuda, T., Aika, Y., Heizmann, C.W., Emson, P.C., Kobayashi, T., Kosaka, T., 1997. Laminar distribution of non-principal neurons in the rat hippocampus, with special reference to their compositional difference among layers. Brain Res. 764, 197–204.
Nunzi, M.G., Gorio, A., Milan, F., Freund, T.F., Somogyi, P., Smith, A.D., 1985. Cholecystokinin-immunoreactive cells form symmetrical synaptic contacts with pyramidal and nonpyramidal neurons in the hippocampus. J. Comp. Neurol. 237, 485–505.
Nyíri, G., Freund, T.F., Somogyi, P., 2001. Input-dependent synaptic targeting of α_2-subunit-containing $GABA_A$ receptors in synapses of hippocampal pyramidal cells of the rat. Eur. J. Neurosci. 13, 428–442.
Ohno-Shosaku, T., Maejima, T., Kano, M., 2001. Endogenous cannabinoids mediate retrograde signals from depolarized postsynaptic neurons to presynaptic terminals. Neuron 29, 729–738.
Pape, H.-C., 1996. Queer current and pacemaker: the hyperpolarization-activated cation current in neurons. Annu. Rev. Physiol. 58, 299–327.
Parker, D., 2000. Presynaptic and interactive peptidergic modulation of reticulospinal synaptic inputs in the lamprey. J. Neurophysiol. 83, 2497–2507.
Parra, P., Gulyás, A.I., Miles, R., 1998. How many subtypes of inhibitory cells in the hippocampus? Neuron 20, 983–993.
Pawelzik, H., Bannister, A.P., Deuchars, J., Ilia, M., Thomson, A.M., 1999. Modulation of bistratified cell IPSPs and basket cell IPSPs by pentobarbitone sodium, diazepam and Zn^{2+}: dual recordings in slices of adult rat hippocampus. Eur. J. Neurosci. 11, 3552–3564.
Pawelzik, H., Hughes, D.I., Bannister, A.P., Thomson, A.M., 2000. Autapses modulate discharge characteristics in hippocampal interneurones. J. Physiol. 526, 60.
Pérez de la Mora, M., Hernandez-Gómez, A.-M., Méndez-Franco, J., Fuxe, K., 1993. Cholecystokinin-8 increases K^+-evoked [^{3}H]γ-aminobutyric acid release in slices from various brain areas. Eur. J. Pharmacol. 250, 423–430.
Peters, A., Miller, M., Kimerer, L.M., 1983. Cholecystokinin-like immunoreactive neurons in rat cerebral cortex. Neuroscience 8, 431–448.
Ramon y Cajal, S., 1893. Estructura del asta de ammon y fascia dentata. Anal. Soc. Espan. Hist. Nat. 22, 53–114.
Ramon y Cajal, S., 1899. Estudios sobre la corteza cerebral humana. Cort. Vis. Rev. Trim. Microgr. 4, 1–63.
Saint, D.A., Buckett, K.J., 1991. Modulation of the transient potassium current in rat hippocampal neurones by cholecystokinin. Neuropeptides 20, 151–157.
Saleh, T.M., Kombian, S.B., Zidichouski, J.A., Pittman, Q.J., 1997. Cholecystokinin and neurotensin inversely modulate excitatory synaptic transmission in the parabrachial nucleus *in vitro*. Neuroscience 77, 23–35.
Savic, N., Pedarzani, P., Sciancalepore, M., 2001. Medium afterhyperpolarization and firing pattern modulation in interneurons of stratum radiatum in the CA3 hippocampal region. J. Neurophysiol. 85, 1986–1997.
Sheehan, M.J., de Belleroche, J., 1983. Facilitation of GABA release by cholecystokinin and caerulein in rat cerebral cortex. Neuropeptides 3, 429–434.
Shinohara, S., Kawasaki, K., 1997. Electrophysiological changes in rat hippocampal pyramidal neurons produced by cholecystokinin octapeptide. Neuroscience 78, 1005–1016.
Sik, A., Penttonen, M., Ylinen, A., Buzsáki, G., 1995. Hippocampal CA1 interneurons: an *in vivo* intracellular labeling study. J. Neurosci. 15, 6651–6665.
Sloviter, R.S., 1989. Calcium-binding protein (calbindin-D_{28k}) and parvalbumin immunocytochemistry: localization in the rat hippocampus with specific reference to the selective vulnerability of hippocampal neurons to seizure activity. J. Comp. Neurol. 280, 183–196.
Solomon, J.S., Nerbonne, J.M., 1993. Two kinetically distinct components of hyperpolarization-activated current in rat superior colliculus-projecting neurons. J. Physiol. 469, 291–313.
Somogyi, P., 1977. A specific 'axo-axonal' interneuron in the visual cortex of the rat. Brain Res. 136, 345–350.
Somogyi, P., Cowey, A., 1981. Combined Golgi and electron microscopic study on the synapses formed by double bouquet cells in the visual cortex of the cat and monkey. J. Comp. Neurol. 195, 547–566.
Somogyi, P., Hodgson, A.J., Smith, A.D., Nunzi, M.G., Gorio, A., Wu, J.-Y., 1984. Different populations of GABAergic neurons in the visual cortex and hippocampus of cat contain somatostatin- or cholecystokinin-immunoreactive material. J. Neurosci. 4, 2590–2603.
Somogyi, P., Tamás, G., Lujan, R., Buhl, E.H., 1998. Salient features of synaptic organisation in the cerebral cortex. Brain Res. Rev. 26, 113–135.
Stella, N., Schweitzer, P., Piomelli, D., 1997. A second endogenous cannabinoid that modulates long-term potentiation. Nature 388, 773–778.
Storm, J.F., 1987. Action potential repolarization and a fast after-hyperpolarization in rat hippocampal pyramidal cells. J. Physiol. 385, 733–759.
Storm, J.F., 1989. An after-hyperpolarization of medium duration in rat hippocampal pyramidal cells. J. Physiol. 409, 171–190.
Szentágothai, J., 1975. The 'module-concept' in cerebral cortex architecture. Brain Res. 95, 475–496.
Szentágothai, J., 1978. The neuron network of the cerebral cortex: a functional interpretation. The Ferrier Lecture, 1977. Proc. R. Soc. London B. 201, 219–248.
Tamás, G., Buhl, E.H., Somogyi, P., 1997. Massive autaptic self-innervation of GABAergic neurons in cat visual cortex. J. Neurosci. 17, 6352–6364.
Tecott, L.H., Maricq, A.V., Julius, D., 1993. Nervous system distribution of the serotonin 5-HT_3 receptor mRNA. Proc. Natl. Acad. Sci. USA 90, 1430–1434.
Thomson, A.M., Bannister, A.P., Hughes, D.I., Pawelzik, H., 2000. Differential sensitivity to Zolpidem of IPSPs activated by morphologically identified CA1 interneurons in slices of rat hippocampus. Eur. J. Neurosci. 12, 425–436.
Tóth, K., Freund, T.F., 1992. Calbindin D_{28k}-containing nonpyramidal cells in the rat hippocampus: their immunoreactivity for GABA and projection to the medial septum. Neuroscience 49, 793–805.
Tsou, K., Mackie, K., Sañudo-Peña, M.C., Walker, J.M., 1999. Cannabinoid CB1 receptors are localized primarily on cholecystokinin-containing GABAergic interneurons in the rat hippocampal formation. Neuroscience 93, 969–975.
Tsubokawa, H., Ross, W.N., 1996. IPSPs modulate spike backpropogation and associated $[Ca^{2+}]_i$ changes in the dendrites of hippocampal CA1 pyramidal neurons. J. Neurophysiol. 76, 2896–2906.
Vida, I., Halasy, K., Szinyei, C., Somogyi, P., Buhl, E.H., 1998. Unitary IPSPs evoked by interneurons at the stratum radiatum-stratum lacunosum-moleculare border in the CA1 area of the rat hippocampus *in vitro*. J. Physiol. 506, 755–773.
Wank, S.A., 1995. Cholecystokinin receptors. Am. J. Physiol. 269, G628–G646.
Williams, S., Samulack, D.D., Beaulieu, C., Lacaille, J.-C., 1994. Membrane properties and synaptic responses of interneurons located near the stratum lacunosum-moleculare/radiatum border of area CA1 in whole-cell recordings from rat hippocampal slices. J. Neurophysiol. 71, 2217–2235.
Williamson, A., Alger, B.E., 1990. Characterization of an early afterhyperpolarization after a brief train of action potentials in rat hippocampal neurons *in vitro*. J. Neurophysiol. 63, 72–81.
Wilson, R.I., Nicoll, R.A., 2001. Endogenous cannabinoids mediate retrograde signalling at hippocampal synapses. Nature 410, 588–591.

Womble, M.D., Moises, H.C., 1993. Hyperpolarization-activated currents in neurons of the rat basolateral amygdala. J. Neurophysiol. 70, 2056–2065.
Woodruff, G.N., Hill, D.R., Boden, P., Pinnock, R., Singh, L., Hughes, J., 1991. Functional role of brain CCK receptors. Neuropeptides 19 (Suppl.), 45–56.
Zhang, L., McBain, C.J., 1995. Potassium conductances underlying repolarization and after-hyperpolarization in rat CA1 hippocampal interneurones. J. Physiol. 488, 661–672.

(*Accepted* 24 *August* 2001)